Synthesis and therapeutic effect of styrene–maleic acid copolymer-conjugated pirarubicin

Kenji Tsukigawa,[1,2] Long Liao,[1] Hideaki Nakamura,[1,2] Jun Fang,[1,2] Khaled Greish,[1,3] Masaki Otagiri[1,2] and Hiroshi Maeda[1]

[1]Institute for Drug Delivery Science, Sojo University, Kumamoto; [2]Faculty of Pharmaceutical Sciences, Sojo University, Kumamoto, Japan

Correspondence

Hiroshi Maeda or Jun Fang, Institute for Drug Delivery Science, Sojo University, Ikeda 4-22-1, Nishi-ku, Kumamoto 860-0082, Japan.
Tel: +81-96-326-4114; Fax: +81-96-326-3185;
E-mails: hirmaeda@ph.sojo-u.ac.jp; fangjun@ph.sojo-u.ac.jp

[3]Present address: Department of Pharmacology and Toxicology, University of Otago, PO Box 56, Dunedin, 9054 New Zealand

Previously, we prepared a pirarubicin (THP)-encapsulated micellar drug using styrene–maleic acid copolymer (SMA) as the drug carrier, in which active THP was non-covalently encapsulated. We have now developed covalently conjugated SMA-THP (SMA-THP conjugate) for further investigation toward clinical development, because covalently linked polymer–drug conjugates are known to be more stable in circulation than drug-encapsulated micelles. The SMA-THP conjugate also formed micelles and showed albumin binding capacity in aqueous solution, which suggested that this conjugate behaved as a macromolecule during blood circulation. Consequently, SMA-THP conjugate showed significantly prolonged circulation time compared to free THP and high tumor-targeting efficiency by the enhanced permeability and retention (EPR) effect. As a result, remarkable antitumor effect was achieved against two types of tumors in mice without apparent adverse effects. Significantly, metastatic lung tumor also showed the EPR effect, and this conjugate reduced metastatic tumor in the lung almost completely at 30 mg/kg once i.v. (less than one-fifth of the maximum tolerable dose). Although SMA-THP conjugate per se has little cytotoxicity *in vitro* (1/100 of free drug THP), tumor-targeted accumulation by the EPR effect ensures sufficient drug concentrations in tumor to produce an antitumor effect, whereas toxicity to normal tissues is much less. These findings suggest the potential of SMA-THP conjugate as a highly favorable candidate for anticancer nanomedicine with good stability and tumor-targeting properties *in vivo*.

Pirarubicin (4′-*O*-tetrahydropyranyldoxorubicin, THP), a semisynthetic derivative of doxorubicin,[1] is one of the anthracycline antitumor drugs used clinically for treatment of various cancers. Compare to doxorubicin, THP shows rapid intracellular uptake,[2] little cardiac toxicity,[3] as well as applicability to doxorubicin-resistant cell lines.[4] However, like many other low molecular weight (MW) antitumor drugs, THP has poor tumor targeting properties, which leads to adverse effects and limits its dosage. Development of drugs with better tumor targeting capability is vital to overcome this drawback.

We have reported that macromolecular drugs (>40 kDa) showed much longer blood circulation and selective tumor accumulation by the enhanced permeability and retention (EPR) effect.[5,6] For this strategy, in our laboratory, styrene–maleic acid copolymer (SMA), an amphiphilic polymer, was used that can encapsulate low MW drugs to spontaneously form micelles.[7,8] Previously we prepared THP-encapsulated SMA micelles by a non-covalent interaction between styrene residues of SMA and THP.[9]

It was reported that the stability of drug-encapsulated micelles by non-covalent interactions was not adequate, and bursting of micelles and the release of low MW drugs in circulation was a problem.[10,11] However, covalently drug-conju-

gated polymeric drugs showed prolonged blood circulation and higher tumor accumulation than non-covalent micellar drugs.[12–14] Thus, one can achieve both high plasma stability and high tumor delivery by using polymer-conjugated drugs.

In this context, we developed a THP-SMA conjugate with covalent bond for further development. This study explains the preparation of the SMA-THP conjugate, its *in vivo* pharmacokinetic advantages, and its antitumor effects. Most strikingly, the antimetastatic effects of this micelle were also observed.

Materials and Methods

Materials. Pirarubicin was kindly provided by MicroBiopharm Japan (Tokyo, Japan), and SMA anhydride (Mr 1600) was purchased from Sigma-Aldrich Japan (Tokyo, Japan). Trinitrobenzene sulfonic acid (TNBS), BSA, RPMI-1640 medium, DMEM, Evans blue, and other reagents and solvents were purchased from Wako Pure Chemical (Osaka, Japan). Fetal calf serum was obtained from Gibco (Grand Island, NY, USA); MTT was purchased from Dojindo Chemical Laboratories (Kumamoto, Japan). All chemicals of reagent grade were used without purification.

Animals. Male ddY mice (6 weeks of age) and male Sprague–Dawley (SD) rats (6 weeks of age) were purchased
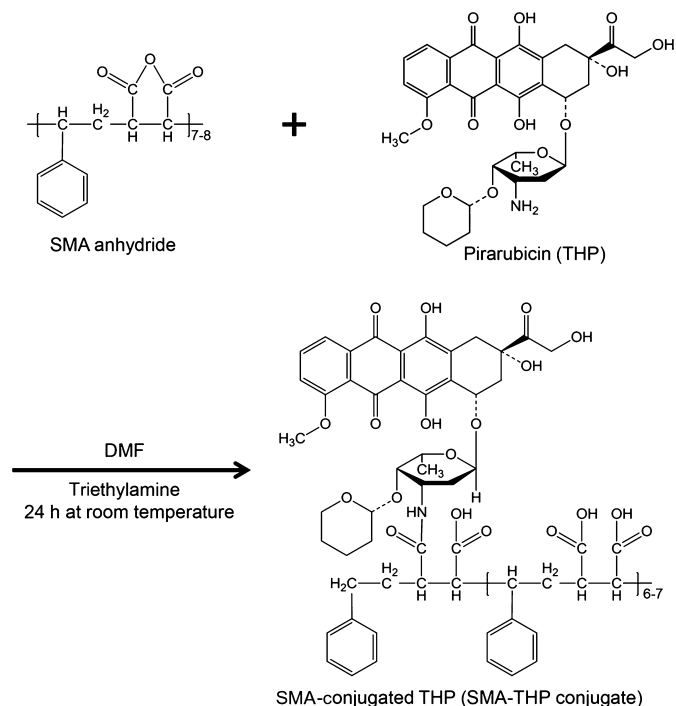
Fig. 1. Synthesis of styrene–maleic acid copolymer (SMA)-conjugated pirarubicin (THP) (SMA-THP conjugate). Chemical structures and conjugation pathway. DMF, *N,N*-dimethylformamide.

from Kyudo (Saga, Japan). Male BALB/cCrSlc mice (6 weeks of age) were purchased from SLC (Shizuoka, Japan).

Synthesis of SMA-THP conjugate. Figure 1 shows a scheme of the synthesis of SMA-THP conjugate. The amino group of THP was used to react with the maleic anhydride residue of SMA to form an amide bond. Briefly, 200 mg SMA anhydride and 100 mg THP were mixed in 10 mL *N,N*-dimethylforma-mide (DMF) followed by addition of 20 μL triethylamine. The reaction was carried out under stirring for 24 h at room temperature in the dark. After the reaction, SMA-THP conjugates were precipitated and washed by diethyl ether, which was then purified by gel permeation chromatography (Bio-Beads SX-1; Bio-Rad, Hercules, CA, USA; $\varphi = 30$ mm, $L = 250$ mm) to remove unreacted THP using DMF as an eluate. Then 0.1 M NaHCO$_3$ (pH 8.2) was added to SMA-THP conjugate to hydrolyze remaining maleic anhydride residues, followed by dialysis against distilled water and ultrafiltration (Millipore, Bedford, MA, USA) with a 50-kDa cut-off membrane, and then lyophilization.

The TNBS method was used to quantify amino groups in SMA-THP conjugate. The THP content in this conjugate was quantified by the absorbance of THP at 480 nm spectrophotometrically.

High performance liquid chromatography. High performance liquid chromatography was carried out by using the LC-2000Plus series HPLC system (JASCO, Tokyo, Japan) equipped with a PU-2080 pump, UV-2075 UV/visible detector, and 807-IT integrator. Multimode size exclusion chromatography was carried out using an Asahipak GF-310 HQ column (7.5 × 300 mm) (Showa Denko, Tokyo, Japan). The mobile phase used DMF at a flow rate of 0.5 mL/min; eluate was monitored at 480 nm for THP.

Sephacryl S-200 size exclusion chromatography. Size exclusion chromatography with Sephacryl S-200 (GE Healthcare, Tokyo,

Japan) was carried out with 0.01 M phosphate buffered 0.15 M saline (PBS, pH 7.4) (column, $\varphi = 15$ mm, $L = 700$ mm).

Dynamic light scattering and zeta potential. The SMA-THP conjugate was dissolved in PBS (pH 7.4) at 2 mg/mL and filtered through a 0.2-μm filter. Particle size and surface charge (zeta potential) were measured by light scattering (ELS-Z2; Photal Otsuka Electronics, Osaka, Japan).

Fluorescence spectroscopy. The SMA-THP conjugate was dissolved in PBS at 10 μg/mL containing various concentration of SDS (0.05–5%) or urea (5–9 M), and fluorescence spectra were recorded with a fluorescence spectrophotometer (FP-6600; JASCO) with excitation at 480 nm and emissions between 500 and 700 nm.

***In vitro* cytotoxicity assay.** HeLa cells (human cervical cancer) were maintained in DMEM supplemented with 10% FCS. Colon 26 cells (mouse colorectal cancer) were maintained similarly but in RPMI-1640 medium.

Cells (3000 cells/well) were plated in 96-well plates (Corning, Corning, NY, USA). After overnight incubation, free THP or SMA-THP conjugate was added. After a further 72 h of culture, MTT assay was carried out to quantify the viable cells.

Intracellular uptake and release of free THP. HeLa cells (5×10^5 cells/well) were placed in a 12-well plate (Corning). After overnight preincubation, cells were treated with free THP or SMA-THP conjugate at 300 μM THP equivalent for indicated times. Cells were then washed twice with PBS, trypsinized, and resuspended in 500 μL methanol (60%) containing 2 M HCl, after which cells were sonicated (30 W for 30 s; Hielscher, Teltow, Germany) and incubated at 50°C for 1 h to hydrolyze THP derivatives, which were extracted by chloroform and quantified by fluorescence intensity (excitation, 480 nm; emission, 590 nm).

To measure the release of free THP, HPLC analysis was carried out. HeLa cells (2×10^6 cells) were placed in a cell culture dish ($\varphi = 60$ mm; Corning). After overnight preincubation, cells were treated with free THP or SMA-THP conjugate at 300 μM THP equivalent for indicated times. Cells were washed twice with PBS, trypsinized, and resuspended in 300 μL DMF, then sonicated in ice-chilled conditions, followed by centrifugation to remove insoluble debris. The supernatant was then subjected to HPLC as described above.

Pharmacokinetics and tissue distribution. All animal experiments were carried out according to the Laboratory Protocol for Animal Handling of Sojo University (Kumamoto, Japan).

Mouse sarcoma S-180 cells (2×10^6 cells) were implanted s.c. in the dorsal skin of male ddY mice. When diameters of the tumors reached approximately 10 mm, 10 mg/kg THP equivalent drugs in saline was injected i.v. into the tail vein. At the indicated time after i.v. injection, mice were killed and perfused with saline followed by removal of each organ. Tissues were dissected, weighed, and methanol (60%) containing 2 M HCl (1 mL per 100 mg tissue) was added for homogenization. Then THP derivatives in the homogenate were measured following the protocol described above.

Similar experiments were also carried out in SD rats (6 weeks of age) to investigate the drug distribution in normal tissues, especially in the lymph nodes (mesenteric lymph nodes) and the bone marrow (from the femoral bone).

***In vivo* antitumor activity of SMA-THP conjugate.** Colon 26 cells (1×10^6 cells) were implanted s.c. in the dorsal skin of male BALB/cCrSlc mice. The S-180 tumor model was prepared as described above. When tumors reached a diameter of approximately 4–6 mm, free THP or SMA-THP conjugate at desired concentrations was administered i.v.. The tumor volume and body weight of the mice were measured during the study

period. Tumor volume (mm^3) was calculated as $(W^2 \times L)/2$ by measuring the width (W) and length (L) of the tumor.

Lung metastasis is known to occur in the colon 26 tumor model.[15,16] Thus we also investigated the antimetastatic effect of SMA-THP conjugate in this model. Namely, on day 50 after tumor inoculation in the dorsal skin (40 days after the treatment described above), Evans blue at 10 mg/kg in saline (0.1 mL) was injected i.v.. After 24 h, mice were killed, perfused with saline, and the lung was excised. Metastatic lung tumors were observed as blue tumor nodules macroscopically and the number of metastatic nodules was counted.

Toxicity of SMA-THP conjugate. Male ddY mice were used to evaluate toxicity of SMA-THP conjugate. Free THP (5 mg/kg, almost maximum tolerable dose [MTD]) was injected i.v. only once, and SMA-THP conjugate was injected i.v. on days 1 and 3 at doses of 10 or 30 mg/kg THP equivalent. The doses were the same as those used in treatment of S-180 tumors. At 36 h and 1 and 2 weeks after the last drug administration, mice were killed and blood samples were obtained to evaluate hematology (white blood cells [WBC], red blood cells [RBC], and hemoglobin levels) and liver, heart, and kidney functions: aspartate aminotransferase, alanine aminotransferase, lactate dehydrogenase, creatine kinase, blood urea nitrogen, and total creatine values.

Statistical analyses. Data were analyzed using ANOVA followed by the Bonferroni multiple comparison test. A difference was considered statistically significant when $P < 0.05$.

Results

Synthesis of SMA-THP conjugate. From 200 mg SMA and 100 mg THP, 225 mg SMA-THP conjugate was obtained, with a THP loading of 30% (w/w), suggesting that the ratio of SMA and THP in the conjugate is approximately one THP/SMA chain. The HPLC analyses showed that SMA-THP conjugate was clearly larger than free THP, and neither free THP nor decomposition product was detected (Fig. 2a). The HPLC analysis using the Capcell Pak C18 column (Type MG, 5 μm, 4.6 mm internal diameter [I.D.] × 250 mm; Shiseido Fine Chemicals, Tokyo, Japan) with 1% acetic acid:acetonitrile mixture (1:1) as eluate also showed that SMA-THP conjugate did not contain unconjugated free THP (Fig. S1). The TNBS assay showed there was no amino group left in SMA-THP conjugate (Fig. 2b). Moreover, SMA-THP conjugate showed better water solubility than free THP, that is, more than 150 mg/mL (45 mg/mL THP) in PBS.

Micelle formation and albumin binding of SMA-THP conjugate in aqueous solution. Dynamic light scattering analysis of SMA-THP conjugate showed that the hydrodynamic diameter was 18.9 ± 10.0 nm (Fig. 2c), which means the conjugate existed in associated form as a micelle in PBS. The zeta potential of the micelle was −32.38 mV in PBS, in contrast to approximately −50 mV unreacted SMA (data not shown).

In aqueous solution, the fluorescence of SMA-THP conjugate was suppressed to approximately 15% of free THP. It was restored by adding SDS (Fig. 2d) or urea (Fig. 2e) to some extent, suggesting that THP on the SMA chain may be interacting with aromatic molecules of styrene residues, forming π−π interaction, and it may be tightly packed inside the micelle.

Size exclusion chromatography using Sephacryl S-200 showed the apparent size of SMA-conjugated THP in PBS was 62 kDa (Fig. 2f,g), which shows as a discrete single peak in the light scattering profile (cf. Fig. 2c) as a single entity (Fig. 2f, SMA-THP conjugate alone [no BSA]).

One noteworthy property of SMA is its albumin binding capacity,[17] which was also supported by the present study. Namely, SMA-THP conjugate behaved like larger molecules in the presence of BSA in a BSA dose-dependent manner, mostly forming a complex of 140 kDa at the BSA concentration of 10 mg/mL (Fig. 2f). In addition, quenching of fluorescence in SMA-THP conjugate was not affected in the presence of BSA (data not shown), which indicates that the conjugate may interact with albumin without disturbing the micellar structure, that is, SMA-THP conjugates bind to albumin as polymeric micelles.

***In vitro* cytotoxicity and intracellular uptake of SMA-THP conjugate, and release of free THP.** As shown in Figure 3(a), SMA-THP conjugate showed dose-dependent cytotoxicity against HeLa cells with an IC$_{50}$ of 22 μM. In contrast, free THP showed much potent cytotoxicity (IC$_{50}$, 0.17 μM). Similar results were observed in colon 26 cells: the IC$_{50}$ of free THP was 0.02 μM, compared to SMA-THP of 12.6 μM (Fig. 3b). In both cell lines, cytotoxicity of SMA-THP conjugate was less than 1/100 compared with that of free THP.

In parallel with these findings, SMA-THP conjugate showed much slower intracellular uptake than free THP, that is, uptake of SMA-THP conjugate at 120 min after treatment was approximately 1/40 that of free THP (Fig. 3c).

Figure 3(d-i) shows the HPLC analysis of free THP taken up into HeLa cells at 6 h after treatment. When cells were treated with SMA-THP conjugate, no free THP but only SMA-THP conjugate was detected in cells (Fig. 3d-ii). Even after 40 h of incubation, release of free THP was not observed in cells (Fig. 3d-iii). At 40 h, death of some HeLa cells was observed.

Pharmacokinetics and tissue distribution of SMA-THP conjugate after i.v. injection. As shown in Figure 4(a), free THP was cleared rapidly from blood circulation after i.v. injection, whereas SMA-THP conjugate remained high in blood circulation for a much longer time, with a 24.5-fold higher concentration curve than free THP. At 24 h after i.v. injection (Fig. 4b), free THP showed the highest concentration in spleen, followed by liver; the accumulation in tumor was very low, at approximately 13% of that in spleen. Accumulation of SMA-THP conjugate was highest in liver, while drug levels in tumor were higher than most other normal tissues. The high accumulation in liver is similar to previous SMA-conjugated drugs (e.g. SMANCS) as well as other macromolecular drugs, mostly through the reticuloendothelial system (e.g. macrophages).[5,18] In addition, high accumulation of SMA-THP conjugate in kidney was also observed, which is probably due to the disintegrated chemical unit of SMA-THP conjugate from micelles whose molecular size (approximately 2200) is smaller than the renal threshold (40 kDa).

It should be noted that the tumor accumulation of SMA-THP conjugate increased to 8.4 times higher than that of free THP. Moreover, the concentration of SMA-THP conjugate in liver, spleen, and kidney decreased gradually and the concentrations were 24.5%, 27%, and 19% at 72 h compared with those at 24 h, respectively (Fig. 4c). In contrast, the concentration of SMA-THP conjugate in tumor at 72 h remained at 75% of that at 24 h, which was the highest concentration, followed by liver, spleen, and kidney (Fig. 4c).

Tissue distribution was also examined using healthy male SD rats. At 24 h after i.v. injection, levels of SMA-THP conjugate in plasma and liver were significantly higher than that of free THP (Fig. 4d). However, no or minimal accumulation of SMA-THP was found in brain, lung, and stomach compared
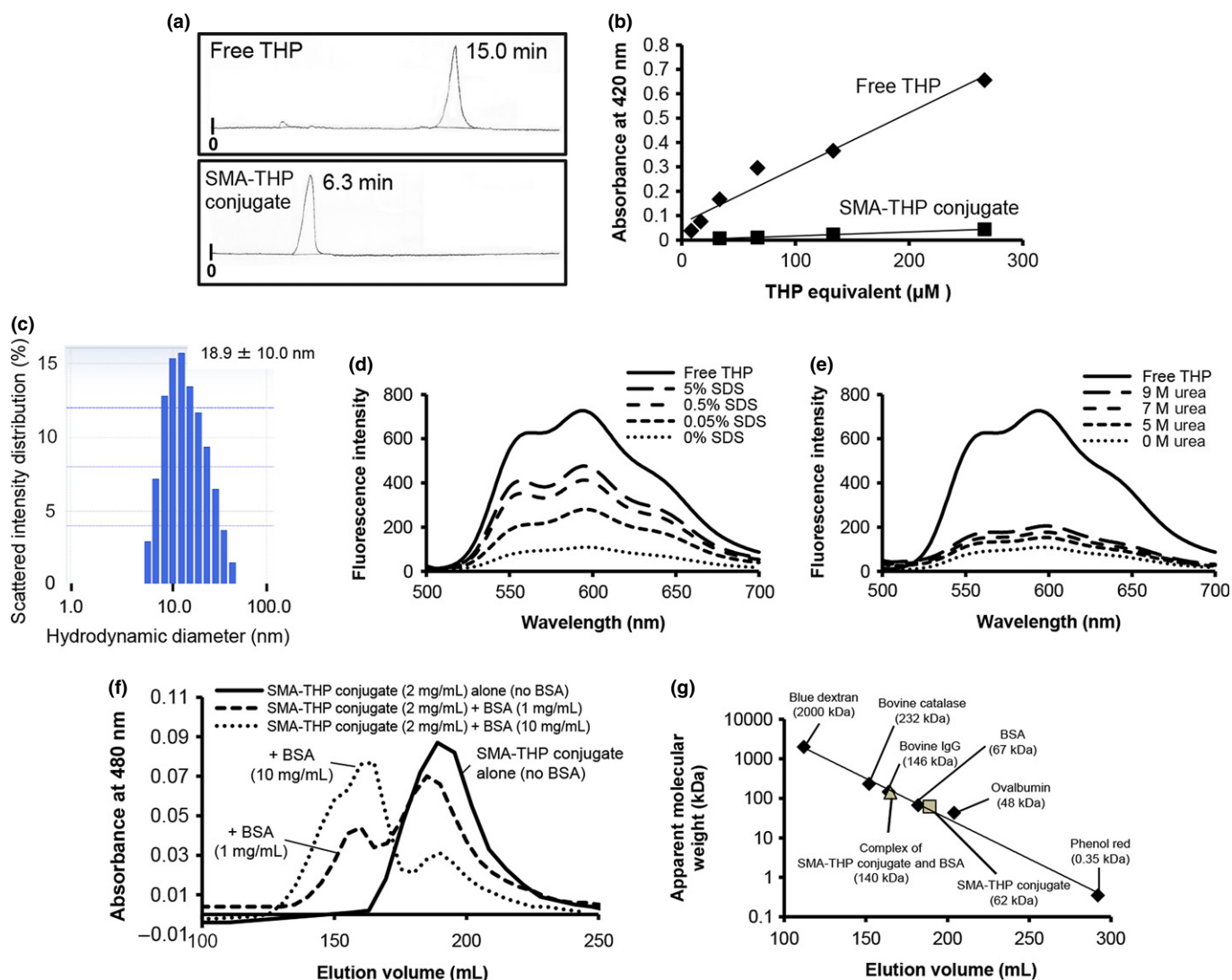
Fig. 2. Characterization of styrene–maleic acid copolymer (SMA)-conjugated pirarubicin (THP) (SMA-THP conjugate). (a) HPLC analyses. (b) Quantification of free amino group by trinitrobenzene sulfonic acid method. (c) Hydrodynamic diameter in PBS of SMA-THP conjugate by dynamic light scattering. (d, e) Fluorescence spectra of SMA-THP conjugate. (f, g) Size exclusion chromatography of SMA-THP conjugate in the presence of different concentrations of BSA by using Sephacryl S-200. The apparent molecular weight of SMA-THP conjugate in the presence /absence of BSA was calculated by the calibration curve based on partition coefficient (K_{av}) using molecular weight standard markers.

with free THP. In other tissues, no significant differences were observed between free THP and SMA-THP conjugate.

Similar to findings in S-180 bearing mice, accumulation of this conjugate in normal tissues including liver, kidney, and bone marrow decreased very rapidly from 24 to 72 h (Fig. 4e).

***In vivo* therapeutic effects against primary tumor and metastasis.** As shown in Figure 5(a), SMA-THP conjugate suppressed tumor growth in a dose-dependent manner, but no decreases in body weight of mice were observed. Free THP at 5 mg/kg, which is close to the MTD, also showed antitumor effects, but body weight loss was significant (Fig. 5b).

More importantly, reduction of metastasis in the lung by SMA-THP conjugate (Fig. 5c,d) was remarkable. As shown in Figure 5(c), in untreated control mice numerous metastatic lung tumor nodules were observed that were stained by Evans blue albumin according to the EPR effect. Treatment with SMA-THP conjugate (30 mg/kg THP equivalent) virtually abolished these lung metastasis (Fig. 5d). In contrast, treatment with free THP (5 mg/kg) showed no apparent effect on lung

metastasis. In addition, at 10 days after tumor inoculation and the start of treatment, no obviously visible tumor nodules were found in lungs of mice (data not shown).

Similar therapeutic effects were also seen in the S-180 tumor model (Fig. 6a,b). We observed apparent cure of tumors in three out of five mice by both doses of the conjugate without recurrence longer than 120 days after tumor inoculation (Fig. 6c).

Toxicity of SMA-THP conjugate. After single injections of the conjugate at different doses (50, 100, or 150 mg/kg THP equivalent ×1), body weight loss was only observed at the dose of 150 mg/kg several days after injection (Fig. 6d). That loss was restored later, however, suggesting that the MTD may be higher than 150 mg/kg, 30 times higher than that of free THP. When free THP was injected twice into S-180 tumor-bearing ddY mice at 10 mg/kg, all mice died within 1 week of the last injection. In colon 26 tumor-bearing BALB/cCrSlc mice, free THP injected once at 5 mg/kg induced continuous decrease of body weight for several days (cf. Fig. 5b).
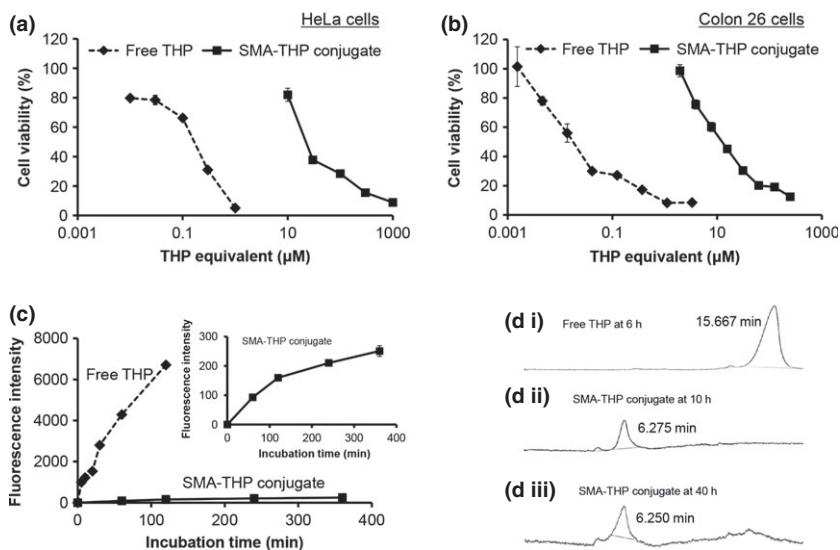
Fig. 3. *In vitro* cytotoxicity and intracellular uptake of free pirarubicin (THP) and styrene–maleic acid copolymer (SMA)-conjugated THP (SMA-THP conjugate). Cytotoxicities of free THP and SMA-THP conjugate against HeLa cells (a) and colon 26 cells (b) were measured by MTT assay. Values are means ± SEM. (c) Intracellular uptake of free THP and SMA-THP conjugate in HeLa cells. Values are means ± SEM ($n = 3$). (d) HPLC analyses of free THP at 6 h (d-i), SMA-THP conjugate at 10 h (d-ii), and 40 h (d-iii) in HeLa cells after each treatment.
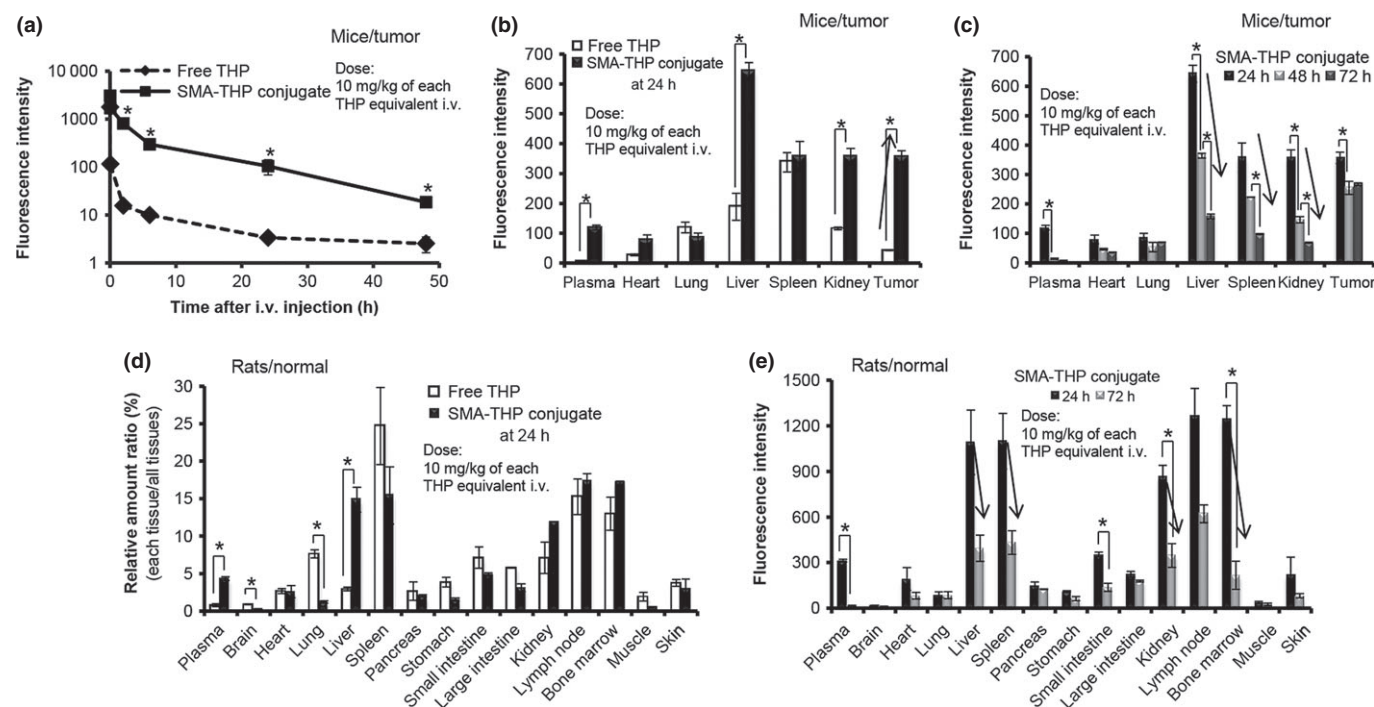

Fig. 4. Pharmacokinetics of free pirarubicin (THP) and styrene–maleic acid copolymer (SMA)-conjugated THP (SMA-THP conjugate) after i.v. injection. (a) Blood levels of both drugs after injection in an S-180 tumor model. (b, c) Tissue distribution of free THP and/or SMA-THP conjugate after i.v. injection in an S-180 tumor model. (d) Relative tissue distribution at 24 h after i.v. injection of free THP and SMA-THP conjugate in healthy SD rats. (e) Comparison of tissue distribution of SMA-THP conjugate at 24 and 72 h after i.v. injection in SD rats. Values are mean ± SEM ($n = 3$). *$P < 0.05$.

In addition, as shown in Table 1, no apparent changes in WBC and RBC counts, hemoglobin levels, or kidney function were found after i.v. injection of 10 and 30 mg/kg SMA-THP conjugate. However, a significant suppression of RBC and hemoglobin levels was observed 1 and 2 weeks after free THP treatment (5 mg/kg ×1). There was slight increase in aspartate aminotransferase after injection of SMA-THP conjugate (30 mg/kg ×2), which might be caused by high accumulation of the conjugate in liver, as revealed by the distribution study (cf. Fig. 3b). Another point to note was that the higher dose of SMA-THP conjugate (30 mg/kg THP equivalent ×2) induced

a weak increase of creatine kinase at 36 h after injection. The increases were dose-dependent but lower than those induced by free THP.

Discussion

In the present study, we prepared an SMA-THP conjugate in which all THP residues were covalently conjugated to the SMA chain, for achieving better circulation stability and tumor-targeting ability (Fig. 1). During preparation, SMA-THP conjugate was purified by use of column chromatography with
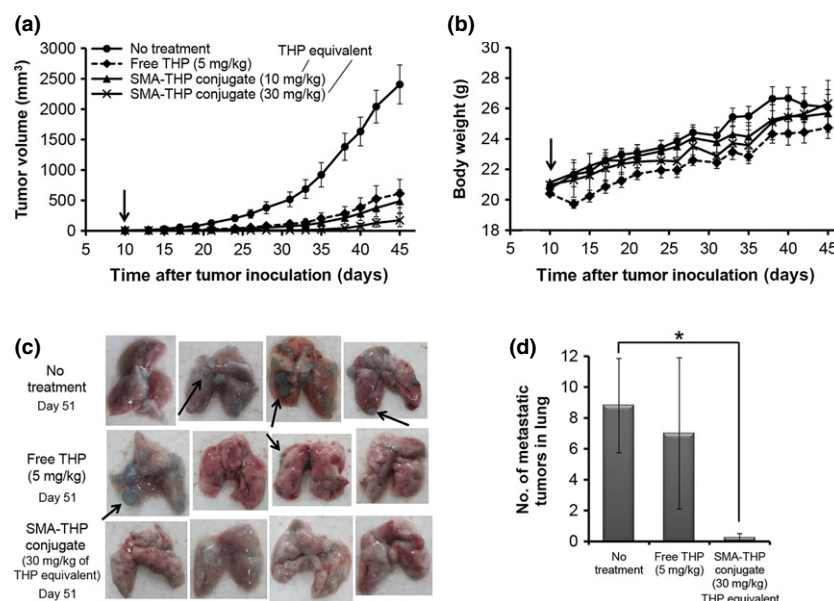
Fig. 5. Effect of styrene–maleic acid copolymer (SMA)-conjugated pirarubicin (THP) (SMA-THP conjugate) on growth and lung metastasis in a colon 26 tumor model. Values are means ± SEM (*n* = 4–5). (a) Antitumor effect. (b) Body weight change in mice after treatment. Vertical arrows indicate injection time of drugs. Figure key shown in (a) also applies to (b). (c) Lung specimens in colon 26 tumor-bearing mice on day 51 after tumor inoculation. Arrows indicate metastatic tumors, quantified as shown in (d). *P < 0.05.
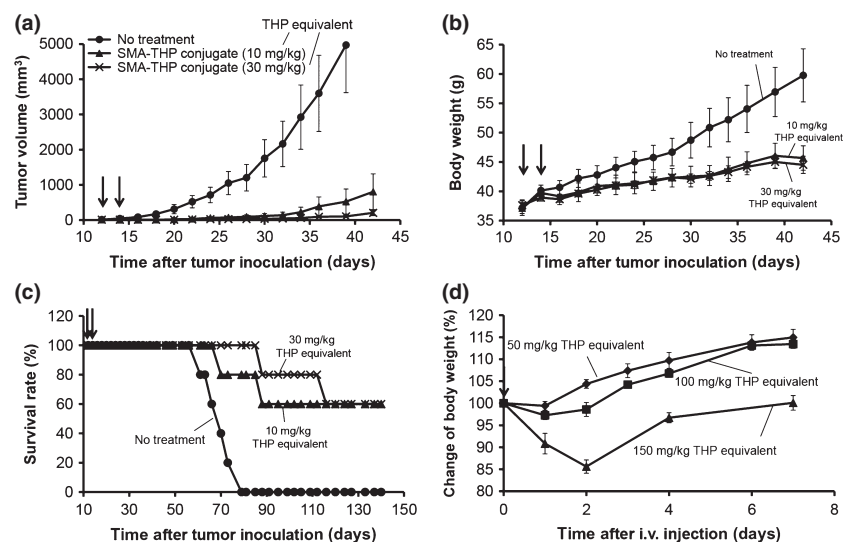
Fig. 6. Antitumor effect of styrene–maleic acid copolymer (SMA)-conjugated pirarubicin (THP) (SMA-THP conjugate) against S-180 tumor. Vertical arrows indicate injection time of drugs. Values are means ± SEM (*n* = 5). (a) Antitumor effect. (b) Body weight change of ddY mice after treatment. (c) Survival rate of S-180 tumor-bearing ddY mice after treatment. Figure key shown in (a) also applies to (b) and (c). (d) Percent change of body weight of healthy normal male ddY mice after injection of different doses of SMA-THP conjugate.

DMF to remove non-covalently bound THP, whereas such low MW drugs encapsulated in micelles cannot be removed in an aqueous column system.

Results of dynamic light scattering (Fig. 2c) and Sephacryl S-200 chromatography (Fig. 2f) suggested that SMA-THP conjugate behaved more similarly to much larger macromolecules in aqueous solution (φ = approximately 19 nm; 62 kDa) than its chemical unit (SMA [1600] + THP [627]). These findings indicate that several SMA-THP conjugates are associated tightly to form a micelle structure, also evidenced by fluorescence quenching of SMA-THP conjugate (Fig. 2d,e). This emergence of fluorescence phenomenon was similarly observed in drug-encapsulated SMA micelles previously developed in our laboratory.[8,9]

Moreover, SMA-THP conjugate was found to bind with BSA, thus behaving as a much larger molecule (Fig. 2f), with an apparent size of 140 kDa (Fig. 2g). The albumin binding capacity of SMA is important for prolonged blood circulation

of SMA-modified drugs, which also confers higher biocompatibility.[17,19] Because albumin is abundant in blood, it is expected that most SMA-THP conjugate exists as a complex with albumin *in vivo*, which consequently led to remarkably prolonged circulation time and much higher tumor accumulation by the EPR effect, compared to free THP (Fig. 4a,b). In addition, although SMA-THP conjugate in normal tissues such as liver, kidney, and bone marrow was cleared time-dependently (Fig. 4c,e); it showed superior accumulation and retention in tumor tissue. These properties then resulted in the remarkable *in vivo* antitumor effect of SMA-THP conjugate without apparent toxicity (Figs 5,6), which was also supported by the results of hematology examination and liver, heart, and kidney functions (Table 1).

The *in vitro* cytotoxicity of SMA-THP conjugate was lower than 1/100 of free THP (Fig. 3a,b), which may be partly related to the lower intracellular uptake of SMA-THP conjugate compared to free THP (Fig. 3c). Moreover, SMA-THP

Table 1. Effect of free pirarubicin (THP) and styrene–maleic acid copolymer (SMA)-conjugated THP (SMA-THP conjugate) on hematology and liver, heart, and kidney functions

Dose of drugs	Time after i.v. administration	WBC (10²/μL)	RBC (10⁴/μL)	Hb (g/dL)	AST (U/L)	ALT (U/L)	LDH (U/L)	CK (U/L)	BUN (mg/dL)	CRE (mg/dL)
Control (no drug)		67.0 ± 12.7	1017.3 ± 31.0	15.2 ± 0.3	32.3 ± 2.0	26.3 ± 2.3	170.3 ± 19.5	40.0 ± 5.6	31.4 ± 2.9	0.11 ± 0.01
Free THP†	36 h	42.5 ± 4.7	971.8 ± 22.0	14.8 ± 0.3	48.3 ± 5.9	33.3 ± 2.2	214.3 ± 29.3	126.3 ± 18.9*	26.1 ± 1.2	0.11 ± 0.01
(5 mg/kg ×1) i.v.	1 week	59.3 ± 13.4	844.5 ± 45.1*	12.7 ± 0.7*	50.0 ± 5.5*	29.5 ± 4.7	366.5 ± 115.7	77.8 ± 10.5*	24.5 ± 3.9	0.12 ± 0.01
	2 weeks	60.7 ± 6.9	926.0 ± 10.6*	13.7 ± 0.5	40.0 ± 4.0	26.3 ± 1.5	233.0 ± 35.1	54.7 ± 10.5	28.5 ± 3.5	0.12 ± 0.02
SMA-THP conjugate‡	36 h	70.3 ± 3.4	967.8 ± 22.0	14.9 ± 0.2	52.3 ± 8.1	43.0 ± 12.7	200.3 ± 26.1	79.0 ± 22.0	32.8 ± 1.9	0.13 ± 0.01
(10 mg/kg THP	1 week	67.3 ± 12.0	960.0 ± 15.3	14.4 ± 0.4	42.3 ± 3.8	31.7 ± 2.2	217.7 ± 12.8	70.0 ± 13.9	24.7 ± 0.8	0.09 ± 0.00
equivalent ×2) i.v.	2 weeks	71.3 ± 9.5	997.0 ± 43.7	15.1 ± 0.2	38.7 ± 3.2	29.7 ± 2.2	157.7 ± 6.4	63.7 ± 21.3	22.1 ± 1.8	0.09 ± 0.00
SMA-THP conjugate§	36 h	47.0 ± 9.0	926.5 ± 55.5	14.4 ± 0.5	70.0 ± 6.8*	36.0 ± 5.4	209.5 ± 29.2	82.0 ± 5.3*	26.2 ± 3.1	0.12 ± 0.01
(30 mg/kg THP	1 week	55.3 ± 1.8	964.0 ± 23.4	14.1 ± 0.5	45.3 ± 0.9*	27.7 ± 1.9	196.3 ± 14.9	51.3 ± 2.8	28.3 ± 1.6	0.10 ± 0.01
equivalent ×2) i.v.	2 weeks	78.7 ± 9.9	1002.7 ± 25.7	14.9 ± 0.4	46.3 ± 3.8*	31.3 ± 0.9	211.3 ± 35.9	58.0 ± 8.0	26.7 ± 1.3	0.11 ± 0.01

Values are means ± SEM ($n = 4$). *$P < 0.05$, significant differences from untreated control group, according to Student's t-test. †Free THP was given i.v. once only; THP at 5 mg/kg is about maximum tolerable dose. ‡10 mg/kg THP equivalent was given i.v. twice, on days 1 and 3. Total dose was 20 mg/kg THP equivalent. §30 mg/kg THP equivalent was given i.v. twice, on days 1 and 3. Total dose was 60 mg/kg THP equivalent. Blood analyses were carried out at 36 h and 1 and 2 weeks after last drug administration. ALT, alanine aminotransferase; AST, aspartate aminotransferase; BUN, blood urea nitrogen; CK, creatine kinase; CRE, creatine; Hb, hemoglobin; LDH, lactate dehydrogenase; RBC, red blood cells; WBC, white blood cells.

conjugate was taken up into HeLa cells as the intact conjugate form and release of free THP from this conjugate did not occur in cells at least 40 h after treatment (Fig. 3d-ii,iii), which may also be partly responsible for the lower cytotoxicity of SMA-THP conjugates. These findings suggested that SMA-THP conjugate per se might show antitumor activity without release of free THP. These results are consistent with previously published reports showing that conjugated drugs with no cleavable bond could also exhibit cytotoxic activity,[20] but the polymer-conjugated drugs usually exhibit lower *in vitro* cytotoxicity.[12,21,22] The low cytotoxicity as well as rapid clearance of SMA-THP conjugate from normal tissues (Fig. 4c,e) may contribute to lower levels of damage to normal tissues *in vivo* (Figs 5,6, Table 1). However, high accumulation of SMA-THP in tumor could ensure sufficient drug concentration (e.g. higher than *in vitro* IC$_{50}$) to fulfill antitumor activity.

Regarding the possible mechanisms of action of SMA-THP conjugate, it was reported that albumin was taken up by tumor cells and degraded to generate amino acids and energy in the cells, by which albumin-conjugated drugs were internalized into tumor cells.[23,24] The SMA-THP conjugate might also be taken up into tumor cells together with the uptake of albumin, and it is then detached from albumin through degradation of albumin, followed by the breakdown of micelle formation in tumor cells (e.g. in lysosomes). Recently, we also reported that breakdown of micelles could be facilitated by amphiphilic components of cell membrane, that is, lecithin.[25] Amphiphilic cell membrane components may thus also contribute to the breakdown of micelles of SMA-THP conjugate during internalization into tumor cells. However, SMA-THP conjugate itself, but not the released free THP, is probably responsible for the antitumor effect of SMA-THP in this study; no release of free THP from SMA-THP conjugate was observed even after 40 h of incubation (Fig. 3d-ii,iii).

In cancer treatment, control of metastatic tumors is a significant problem and a major cause of therapeutic failure. Tumor metastases are often invisible and emerge at distant sites, and their response to chemotherapy and radiotherapy is rather inefficient. Under such circumstances, an important finding of the present study is that treatment with SMA-THP conjugate against colon 26 tumors showed not only growth suppression of implanted tumor in dorsal skin, but also almost complete simultaneous eradication of metastatic tumor in lung (Fig. 5).

We previously reported that SMA-conjugated neocarzinostatin SMANCS showed an antilymphatic metastatic effect mostly because of the EPR-based tumor targeting.[26–28] The EPR effect has also been observed in small tumor nodules (e.g. 200 μm in diameter).[29–31] In this study, we also found that Evans blue-bound albumin selectively accumulated in metastatic lung cancers by the EPR effect (Fig. 5c). Polymer-conjugated drugs or macromolecular drugs showing the EPR effect in metastatic tumor is a very intriguing finding in this report. Although no obviously visible lung metastatic tumor nodules were found at 10 days after tumor inoculation and start of treatment, SMA-THP conjugate may accumulate in the small invisible metastatic tumor nodules by the EPR effect, and exert an antimetastatic effect. However, the major cause of decreased metastatic lung tumors by treatment with SMA-THP conjugates is considered to be the consequence of growth suppression of the inoculated primary tumor. Further studies of the effect of SMA-THP conjugate on tumor metastases are warranted.

Conjugation of drugs with SMA is known to confer immunopotentiating effects, such as activation of macrophages,

T cells, and natural killer cells, and induction of interferon.[32–35] Such an effect of SMA-THP conjugate might thus confer another benefit for development of macromolecular antitumor drugs for clinical application.

In conclusion, covalently linked SMA-THP conjugate showed prolonged circulation time and tumor-targeting properties based on the EPR effect. Consequently, marked *in vivo* antitumor effects were achieved against different types of tumor, including metastatic lung cancer, with few adverse effects. Thus, SMA-THP conjugate appears to be a promising candidate for further development, having high *in vivo* stability and tumor-targeting efficiency.

Disclosure Statement

The authors have no conflicts of interest.

References

1 Umezawa H, Takahashi Y, Kinoshita M *et al.* Tetrahydropyranyl derivatives of daunomycin and adriamycin. *J Antibiot (Tokyo)* 1979; **32**: 1082–4.

2 Kunimoto S, Miura K, Takahashi Y, Takeuchi T, Umezawa H. Rapid uptake by cultured tumor cells and intracellular behavior of 4′-O-tetrahydropyranyladriamycin. *J Antibiot (Tokyo)* 1983; **36**: 312–7.

3 Koh E, Ueda Y, Nakamura T, Kobayashi A, Katsuta S, Takahashi H. Apoptosis in young rats with adriamycin-induced cardiomyopathy-comparison with pirarubicin, a new anthracycline derivative. *Pediatr Res* 2002; **51**: 256–9.

4 Kunimoto S, Miura K, Umezawa K *et al.* Cellular uptake and efflux and cytostatic activity of 4′-O-tetrahydropyranyladriamycin in adriamycin-sensitive and resistant tumor cell lines. *J Antibiot (Tokyo)* 1984; **37**: 1697–702.

5 Matsumura Y, Maeda H. A new concept for macromolecular therapeutics in cancer chemotherapy: mechanism of tumoritropic accumulation of proteins and the antitumor agent smancs. *Cancer Res* 1986; **46**: 6387–92.

6 Fang J, Nakamura H, Maeda H. The EPR effect: unique features of tumor blood vessels for drug delivery, factors involved, and limitations and augmentation of the effect. *Adv Drug Deliv Rev* 2011; **63**: 136–51.

7 Greish K, Sawa T, Fang J, Akaike T, Maeda H. SMA-doxorubicin, a new polymeric micellar drug for effective targeting to solid tumours. *J Control Release* 2004; **97**: 219–30.

8 Iyer AK, Greish K, Fang J, Murakami R, Maeda H. High-loading nanosized micelles of copoly(styrene-maleic acid)-zinc protoporphyrin for targeted delivery of a potent heme oxygenase inhibitor. *Biomaterials* 2007; **28**: 1871–81.

9 Greish K, Nagamitsu A, Fang J, Maeda H. Copoly(styrene-maleic acid)-pirarubicin micelles: high tumor-targeting efficiency with little toxicity. *Bioconjug Chem* 2005; **16**: 230–6.

10 Yeo Y, Park K. Control of encapsulation efficiency and initial burst in polymeric microparticle systems. *Arch Pharm Res* 2004; **27**: 1–12.

11 Hasan AS, Socha M, Lamprecht A *et al.* Effect of the microencapsulation of nanoparticles on the reduction of burst release. *Int J Pharm* 2007; **344**: 53–61.

12 Lee SJ, Koo H, Jeong H *et al.* Comparative study of photosensitizer loaded and conjugated glycol chitosan nanoparticles for cancer therapy. *J Control Release* 2011; **152**: 21–9.

13 Kaminskas LM, McLeod VM, Porter CJH, Boyd BJ. Association of chemotherapeutic drugs with dendrimer nanocarriers: an assessment of the merits of covalent conjugation compared to noncovalent encapsulation. *Mol Pharm* 2012; **9**: 355–73.

14 Hollis CP, Weiss HL, Leggas M, Evers BM, Gemeinhart RA, Li T. Biodistribution and bioimaging studies of hybrid paclitaxel nanocrystals: lessons learned of the EPR effect and image-guided drug delivery. *J Control Release* 2013; **172**: 12–21.

15 Iigo M, Nakagawa T, Ishikawa C *et al.* Inhibitory effects of docosahexaenoic acid on colon carcinoma 26 metastasis to the lung. *Br J Cancer* 1997; **75**: 650–5.

16 Suzuki I, Iigo M, Ishikawa C *et al.* Inhibitory effects of oleic and docosahexaenoic acids on lung metastasis by colon-carcinoma-26 cells are associated with reduced matrix metalloproteinase-2 and -9 activities. *Int J Cancer* 1997; **73**: 607–12.

17 Kobayashi A, Oda T, Maeda H. Protein binding of macromolecular anticancer agent SMANCS: characterization of poly(styrene-co-maleic acid) derivatives as an albumin binding ligand. *J Bioact Compat Polym* 1988; **3**: 319–33.

18 Bertrand N, Leroux J-C. The journey of a drug-carrier in the body: an anatomo-physiological perspective. *J Control Release* 2012; **161**: 152–63.

19 Fang J, Seki T, Qin H, Bharate GY, Iyer AK, Maeda H. Tissue protective effect of xanthine oxidase inhibitor, polymer conjugate of (styrene-maleic acid copolymer) and (4-amino-6-hydroxypyrazolo[3,4-d]pyrimidine), on hepatic ischemia-reperfusion injury. *Exp Biol Med (Maywood)* 2010; **235**: 487–96.

20 Malugin A, Kopecková P, Kopecek J. Liberation of doxorubicin from HPMA copolymer conjugate is essential for the induction of cell cycle arrest and nuclear fragmentation in ovarian carcinoma cells. *J Control Release* 2007; **124**: 6–10.

21 Veronese FM, Schiavon O, Pasut G *et al.* PEG-doxorubicin conjugates: influence of polymer structure on drug release, in vitro cytotoxicity, biodistribution, and antitumor activity. *Bioconjug Chem* 2005; **16**: 775–84.

22 Nakamura H, Etrych T, Chytil P *et al.* Two step mechanisms of tumor selective delivery of *N*-(2-hydroxypropyl)methacrylamide copolymer conjugated with pirarubicin via an acid-cleavable linkage. *J Control Release* 2014; **174**: 81–7.

23 Stehle G, Sinn H, Wunder A *et al.* Plasma protein (albumin) catabolism by the tumor itself – implications for tumor metabolism and the genesis of cachexia. *Crit Rev Oncol Hematol* 1997; **26**: 77–100.

24 Kratz F. Albumin as a drug carrier: design of prodrugs, drug conjugates and nanoparticles. *J Control Release* 2008; **132**: 171–83.

25 Nakamura H, Fang J, Gahininath B, Tsukigawa K, Maeda H. Intracellular uptake and behavior of two types zinc protoporphyrin (ZnPP) micelles, SMA-ZnPP and PEG-ZnPP as anticancer agents; unique intracellular disintegration of SMA micelles. *J Control Release* 2011; **155**: 367–75.

26 Maeda H, Takeshita J, Kanamaru R, Sato H, Khatoh J. Antimetastatic and antitumor activity of a derivative of neocarzinostatin: an organic solvent- and water-soluble polymer-conjugated protein. *Gan* 1979; **70**: 601–6.

27 Takeshita J, Maeda H, Kanamaru R. In vitro mode of action, pharmacokinetics, and organ specificity of poly (maleic acid-styrene)-conjugated neocarzinostatin, SMANCS. *Gan* 1982; **73**: 278–84.

28 Ohtsuka N, Konno T, Miyauchi Y, Maeda H. Anticancer effects of arterial administration of the anticancer agent SMANCS with lipiodol on metastatic lymph nodes. *Cancer* 1987; **59**: 1560–5.

29 Daruwalla J, Greish K, Malcontenti-Wilson C *et al.* Styrene maleic acid-pirarubicin disrupts tumor microcirculation and enhances the permeability of colorectal liver metastases. *J Vasc Res* 2009; **46**: 218–28.

30 Daruwalla J, Nikfarjam M, Greish K *et al.* In vitro and in vivo evaluation of tumor targeting styrene-maleic acid copolymer-pirarubicin micelles: survival improvement and inhibition of liver metastases. *Cancer Sci* 2010; **101**: 1866–74.

31 Maeda H. The link between infection and cancer: tumor vasculature, free radicals, and drug delivery to tumors via the EPR effect. *Cancer Sci* 2013; **104**: 779–89.

32 Oda T, Morinaga T, Maeda H. Stimulation of macrophage by polyanions and its conjugated proteins and effect on cell membrane. *Proc Soc Exp Biol Med* 1986; **181**: 9–17.

33 Suzuki F, Pollard RB, Uchimura S, Munakata T, Maeda H. Role of natural killer cells and macrophages in the nonspecific resistance to tumors in mice stimulated with SMANCS, a polymer-conjugated derivative of neocarzinostatin. *Cancer Res* 1990; **50**: 3897–904.

34 Suzuki F, Munakata T, Maeda H. Interferon induction by SMANCS: a polymer-conjugated derivative of neocarzinostatin. *Anticancer Res* 1988; **8**: 97–103.

35 Masuda E, Maeda H. Changes in cellular components of spleen and lymph node cells and the effector cells responsible for Meth A tumor eradication induced by zinostatin stimalamer. *Cancer Res* 1996; **56**: 1868–73.

Supporting Information

Additional supporting information may be found in the online version of this article:

Fig. S1. High performance liquid chromatography analyses using a Capcell Pak C18 column of free pirarubicin (THP) and styrene–maleic acid co-polymer (SMA)-conjugated THP (SMA-THP conjugate).